Well localized crystalline orbitals obtained from Bloch functions: The case of $KNbO_3$

Ph. Baranek,[1] C. M. Zicovich-Wilson,[1,*] C. Roetti,[1] R. Orlando,[1] and R. Dovesi[1,2,†]
[1]*Department CIFM, University of Torino, via Giuria 5, I-10125 Torino, Italy*
[2]*Unità INFM di Torino, Sezione F, via Giuria 5, I-10125 Torino, Italy*
(Received 6 April 2001; published 4 September 2001)

The crystalline orbitals of $KNbO_3$ are localized according to an iterative mixed Wannier-Boys scheme. The transformed orbitals turn out to be extremely localized; their features and degree of localization are described in terms of various indices. The spontaneous polarization and the effective Born charges of the various atoms are evaluated starting from the localized Wannier function (LWF) centroids and from delocalized Bloch functions through the Berry phase (BP) scheme. It turns out that the results provided by both approaches agree very well (for example, the spontaneous polarization is 0.3361 and 0.3347 C/m^2 from the LWF and BP methods, respectively).

DOI: 10.1103/PhysRevB.64.125102 PACS number(s): 77.22.Ej, 71.23.An, 77.84.Dy, 71.15.Nc

I. INTRODUCTION

The crystalline orbitals (CO's) describing the electronic ground state of a periodic system are usually obtained as linear combinations of (delocalized) Bloch functions (BF's), in order to exploit the block factorization of the Hamiltonian matrix, because BF's are bases for irreducible representations of the translation group. Localized Wannier functions (LWF's) can be obtained by applying a unitary transformation to the CO's and different degrees of localization can be obtained depending on the transformation. Transformations that provide very well localized Wannier functions are particularly useful for several reasons (see also the conclusions in Ref. 1).

(i) LWF's permit an easy and intuitive description of the electronic structure of crystalline compounds in terms of chemical concepts, such as lone pairs, shared electrons, and covalent or ionic bonds;

(ii) In terms of these localized states, many properties can be evaluated in an extremely simple and intuitive way, whereas expensive and not easy to implement methods are required, when delocalized CO's are used. This is the case, for example, of the spontaneous polarization (ΔP) and the effective Born charges[2,3] (Z^*), which in the localized representation are nothing else than the difference in the dipole moment of the cell charge distributions evaluated at two different geometries (see below for a more precise definition), whereas in the BF representation they are evaluated through a formalism based on Berry phases[4–7] (BP's) that requires the evaluation of complicated and expensive integrals.

(iii) Well-localized WF's can be used for the implementation of *post* Hartree-Fock estimates of the correlation energy, using the methods either of many-body perturbation[8–10] or configuration interaction or coupled cluster[11,12] theories.

We have implemented a localization scheme that provides extremely localized WF's. It consists in the iteration of a Wannier-type transformation, applied to the subset of bands we are interested in, followed by a Boys-type transformation.[13,14] The method has been presented elsewhere[15] and its efficiency and dependence on all computational parameters have been discussed at length. In the following section we shortly summarize the general features.

The aim of this paper is twofold.

(i) To provide an example of the capabilities of the localization scheme as implemented in our computer program CRYSTAL. The localization scheme will be applied to $KNbO_3$, a ferroelectric material with a perovskitelike structure. The degree of localization of the WF's will be estimated in terms of various localization indices, usually adopted in molecular quantum chemistry.[16,17]

(ii) To evaluate ΔP and Z^* in $KNbO_3$ from the centroids of the LWF's, and compare them with the corresponding quantities obtained from the BP algorithm.[4–7] In principle, both approaches should provide exactly the same results when the same basis set and computational conditions are adopted (a BP option has recently been implemented in the CRYSTAL program[18]). This is true, however, only in the limit of very high accuracy and full convergence with respect to all computational parameters.

II. METHODOLOGICAL ASPECTS

The present calculations have been performed at the Hartree-Fock level with the periodic *ab initio* CRYSTAL code.[19] CRYSTAL uses a variational basis set of BF's obtained from contracted Gaussian-type functions (GTF's). A GTF is the product of a Gaussian (G) times a real solid spherical harmonic. Each contracted GFT, $\varphi_\mu(\mathbf{r}-\mathbf{s}_\mu)$, is usually centered at an atomic site $\mathbf{s}_\mu$, ($\mu=1,\ldots,M$ labels the functions centered in the primitive cell) and it will be referred to as an ''atomic orbital'' (AO) in the following. The CO's so defined take the form

$$\psi_s(\mathbf{r},\mathbf{k})=\sum_{\mu=1}^{M}\alpha_\mu^s(\mathbf{k})\sum_{l=1}^{L}e^{i\mathbf{k}\cdot\mathbf{R}_l}\varphi_\mu(\mathbf{r}-\mathbf{s}_\mu-\mathbf{R}_l), \qquad (1)$$

where the sums run over the M AO's in the reference cell and the L cells of the system (actually $L=\infty$). As regards the atomic basis sets, small core pseudopotentials[20–22] have been used for Nb and K (see Table I). The Nb basis set contains $2sp$ shells ($3G$ and $1G$ contractions) and $2d$ shells ($3G$ and $1G$ contractions). For K, $3sp$ shells (2-1-1 G contractions) have been used. For oxygen, the same all electron basis set as in previous papers (see Refs. 23 and 24) has been adopted;

TABLE I. Exponents and coefficients of the contracted Gaussian basis set adopted in the present study for Nb and K, in conjunction with Hay-Wadt small core pseudopotentials. The coefficients multiply individually normalized Gaussian-type orbitals.

	Niobium			Potassium		
		Coeff.			Coeff.	
Shell	Expt.	$s(d)$	p	Expt.	$s(d)$	p
sp	4.013674	0.310659	−0.241891	7.506000	−0.0209	−0.0495
	2.968789	−1.031337	0.020413	2.371	−0.4292	0.0266
	1.056328	1.044714	1.344745			
sp	0.451074	1.0	1.0	0.913	1.0	1.0
				0.3092	1.0	1.0
d	21.317193	−0.016394				
	1.358360	2.487991				
	0.488781	4.631201				
d	0.210860	1.0				

it contains 18 functions (a contraction of 8, 4, 1, 1, and 1 GTF's for the $1s$, $2sp$, $3sp$, $4sp$, and d shells, respectively). The two outer sp GTF's have been reoptimized ($\alpha_{sp}=0.5$ and 0.215 bohr^{-2}). The d-shell exponent is $\alpha_d=0.6\,\text{bohr}^{-2}$.

The experimental tetragonal unit cell structural parameters measured[25] at 270 °C have been used: $a=3.997$ Å and $c=4.063$ Å. With Nb in the origin the remaining displacements[25] (in fractional units) along the c direction are 0.023 (K), 0.040 (O_I), and 0.042 (O_{II}), where "O_I" labels each of the two oxygen ions along the c axis and "O_{II}" the four oxygen ions in the basal plane of the octahedron.

As regards the computational conditions for the evaluation of the Coulomb and exchange series, the adopted truncation tolerances are 6 8 6 6 17 (see Ref. 19). The shrinking factors of the reciprocal space net, at which the Fock matrix is diagonalized, has been set to 8 corresponding to 75 reciprocal space points. The total energies obtained with this mesh can be considered as fully converged.

A. Localized crystalline orbitals

In the present work the WF's $\omega_s(\mathbf{r})$ are expressed in terms of the AO's as

$$\omega_s(\mathbf{r})=\sum_{\mu=1}^{M}\sum_{l=1}^{L} C^s_{\mu,\mathbf{R}_l}\varphi_\mu(\mathbf{r}-\mathbf{s}_\mu-\mathbf{R}_l). \tag{2}$$

Every set $\{\omega_s(\mathbf{r}-\mathbf{R}_l)\}_{l=1}^{L}$ fulfills the orthonormality condition

$$\int d\mathbf{r}\,\omega_s(\mathbf{r}-\mathbf{R}_l)^*\omega_s(\mathbf{r}-\mathbf{R}_m)=\delta_{lm}, \tag{3}$$

and spans a translationally invariant subspace, which hereafter will be referred to as the s band (note that s simply labels a given band; it does not refer, in general, to a band built with s-type orbitals). The same subspace can also be described in terms of BF's, which are by definition stable under lattice translations [see Eq. (1)].

The coefficients $c^s_{\mu,\mathbf{R}_l}$ and $\alpha^s_\mu(\mathbf{k})$ in Eqs. (1) and (2), respectively, are related by Fourier-like transforms:

$$c^s_{\mu,\mathbf{R}_l}=\frac{V}{(2\pi)^3}\int_{BZ} d\mathbf{k}\,e^{i\mathbf{k}\cdot\mathbf{R}_l}\alpha^s_\mu(\mathbf{k})$$

$$=\frac{1}{L}\sum_{j=1}^{L} e^{i\mathbf{k}_j\cdot\mathbf{R}_l}\alpha^s_\mu(\mathbf{k}_j), \tag{4}$$

$$\alpha^s_\mu(\mathbf{k})=\sum_{l=1}^{L} e^{-i\mathbf{k}\cdot\mathbf{R}_l}c^s_{\mu,\mathbf{R}_l}. \tag{5}$$

In the first equality of Eq. (4), integration is performed over the first Brillouin zone (BZ) and V is the cell volume, while in the second equality the finite approach is used and k_j are the nodes of a Monkhorst-Pack net within the BZ.[26] In this approach the number of points in the net, L, is the same as the number of cells in direct space considered in Eq. (2). Therefore, infinite sums in Eqs. (1), (2), (4), and (5) are in practice restricted to a finite number of terms.

Let us now define the *active* subspace S, which is spanned by a given set of s bands, $s=1,\ldots,N$. Here S can be, for instance, the subspace of the N valence bands obtained from a Hartree-Fock calculation. It was shown in a previous work[1] that for nonconducting systems there exists a set of WF's that span a given S in the occupied space and are maximally localized in coordinate space. Well localized WF's are now obtainable with CRYSTAL at a relatively low computational cost. In the following the method will be introduced briefly, while a complete discussion is reported elsewhere.[15]

The "wannierization" step starts from a guess for the WF's, $\{\omega_s^{(0)}(\mathbf{r})\}_{s=1}^{N}$, which is supplied in input or obtained using heuristic methods. The electron density of the sth WF so obtained, which is assigned to the reference cell [see Eq. (2)] is decomposed into atomic populations $q^s_{A,\mathbf{R}_l}$ of atom A and cell l using Mulliken analysis:

$$q^s_{A,\mathbf{R}_l}=\sum_{\mu\in A}\sum_{\nu,m} c^s_{\mu,\mathbf{R}_l}c^s_{\nu,\mathbf{R}_m+\mathbf{R}_l}S^{\mathbf{R}_m}_{\mu\nu}, \tag{6}$$

where the first sum runs over the AO's at atom A, $S^{R_m}_{\mu\nu}$ is the overlap between the AO's $\varphi_\mu(\mathbf{r}-\mathbf{s}_\mu)$ and $\varphi_\nu(\mathbf{r}-\mathbf{s}_\nu-\mathbf{R}_m)$, and the c^s coefficients are given by Eq. (2). The electron densities are normalized so that

$$\sum_{l=1}^{L}\sum_{A=1}^{P} q^s_{A,\mathbf{R}_l}=1, \tag{7}$$

where the second sum runs over the P atoms in the reference cell.

The Mulliken atomic populations are used to calculate the array G^s_A which provides the lattice vector R_l assigned to the periodic image of atom A, which displays the maximum atomic population in $\omega^{(0)}_s(r)$:

$$\mathbf{G}^s_A=\mathbf{R}_l\leftrightarrow q^s_{A,\mathbf{R}_l}=\max\{q^s_{A,\mathbf{R}_m}\}_m\,. \tag{8}$$

Therefore, $\mathbf{G}^s_A$ denotes the primitive cell (i.e., an irreducible set of atoms not necessarily all in the same lattice cell l) where the sth WF is mainly localized. A new function $\mathcal{F}_s(r)$ (not necessarily a WF) is obtained for each s band considering only the contributions of those AO's that are within the primitive cell defined by $\mathbf{G}^s_A$ in $\omega^{(0)}_s(\mathbf{r})$,

$$\mathcal{F}_s(\mathbf{r})=\sum_{A=1}^{P} p^s_A\sum_{\mu\in A} c^{s,(0)}_{\mu,\mathbf{G}^s_A}\varphi_\mu(\mathbf{r}-\mathbf{s}_\mu-\mathbf{G}^s_A), \tag{9}$$

where the second sum runs over the μ atomic orbitals at atom A and weights p^s_A read

$$p^s_A=\begin{cases}0 & \text{if } q^s_{A,\mathbf{R}_l}<\theta, \quad \forall l=0,\ldots,L-1,\\ 1 & \text{otherwise.}\end{cases} \tag{10}$$

θ is a given threshold, which in the present calculation is set to 10^{-1}. Weights p^s_A are employed to exclude the original WF tails from the model function $\mathcal{F}_s$. Their role in the present localization scheme is briefly discussed below.

The functions $\mathcal{F}_s(r)$ are then retransformed into the BF representation using Eq. (5) and projected onto the active subspace at each $\mathbf{k}_j$ point of the Monkhorst net using the projector

$$P_{\mathbf{k}_j}=\sum_{s=1}^{N}|\psi_s(\mathbf{k}_j)\rangle\langle\psi_s(\mathbf{k}_j)|, \tag{11}$$

where vector notation for the BF $\psi_s(\mathbf{r},\mathbf{k}_j)$, $|\psi_s(\mathbf{k}_j)\rangle$, is used. The projected vectors are then symmetrically orthonormalized at each $\mathbf{k}_j$ and backtransformed into WF's using Eq. (4). Finally, the atomic populations are calculated for each ω_s and, when required, each one is shifted a given lattice vector in order to ensure that most of the electron population is contained within the reference cell. The resulting WF's $\omega^{(1)}_s(\mathbf{r})$ are the input to the next step: the Boys step.

In the Boys step a unitary transformation U_{st} is applied that maximizes the functional Ω_B,

$$\Omega_{\mathbf{B}}=\sum\nolimits_{s<s'}^{N}|\langle\omega^{(2)}_s|\mathbf{r}|\omega^{(2)}_s\rangle-\langle\omega^{(2)}_{s'}|\mathbf{r}|\omega^{(2)}_{s'}\rangle|^2, \tag{12}$$

where $\omega^{(2)}_s(\mathbf{r})=\Sigma^N_{t=1}U_{st}\omega^{(1)}_t(\mathbf{r})$. The computational procedure used to maximize Ω_B is exactly the same as reported for the molecular Foster-Boys method.[13,14] The output WF's $\omega^{(2)}_s(\mathbf{r})$ are then tested for convergence. If convergence is not achieved, the $\omega^{(2)}_s$ are used as a guess in the next ''wannierization'' step and the process continues.

The role of the Boys step consists in refining the localization performed in the previous wannierization step by explicitly introducing a minimization of the most relevant off-diagonal terms in the matrix representation of the $\mathbf{r}$ operator.[1,2,15] The better localized character of the resulting LWF's allows one to define more suitable model functions $\mathcal{F}_s$ to be used in the next iteration, improving efficiency in the next wannierization step. Accordingly, the degree of localization of the WF's is improved at each cycle of the iterative scheme, and, as shown in Ref. 15, the functions obtained at the end of the process can be considered very good approximations to globally optimized LWF's.

Convergence is tested using the so-called atomic delocalization index Λ, which provides a measure of the extent of the WF's in terms of number of atoms,[16]

$$\Lambda=\left[\frac{1}{N}\sum_{s=1}^{N}(\lambda^s)^{-1}\right]^{-1}, \tag{13}$$

where the atomic extent of the single sth WF, λ^s, reads

$$\lambda^s=\left[\sum_{A=1}^{P}\sum_{l=1}^{L}(q^s_{A,\mathbf{R}_l})^2\right]^{-1}. \tag{14}$$

Calculation stops at cycle n if $|\Lambda_n-\Lambda_{n-1}|$ is less than a given tolerance, which in the present case is $10^{-5}e^{-2}$.

Concerning the initial guess needed to start the procedure, it is shown elsewhere[15] that the choice is not critical for ionic systems, as those considered in the present case, and any set of $\mathcal{F}_s$ vectors that fulfill the conditions of being linearly independent and well localized within the reference cell is adequate. In the present work such vectors are obtained from Eq. (9), using $\mathbf{G}^s_A=\mathbf{0}$, $\forall A$, s, and $c^{s,(0)}_{\mu,0}=\mu^s_\mu(\mathbf{0})$, where $\alpha^s_\mu(\mathbf{0})$ are the BF coefficients calculated in the self-consistent field (SCF) step at $\mathbf{k}=\mathbf{0}$.

Let us finally describe shortly the role of threshold θ in Eq. (10). As discussed in Ref. 15, in systems with large unit cells the matrix elements $\mathbf{G}^s_A$ for atoms A in the WF tails may not be correctly assigned by means of Eq. (8) due to the numerical fluctuations in the initial stages of the localization scheme. It is also shown that in such cases, if model functions $\mathcal{F}_s$ are defined considering all the AO contributions in Eq. (9) (i.e., all elements of p^s_A equal to 1), the scheme either diverges or yields loosely localized WF's. On the contrary, by using a suitable value of θ in Eq. (10), the indetermination in the definition of the WF tails is avoided, as the corresponding terms are canceled in Eq. (9); as a result, a good convergence is in practice ensured.

This scheme differs in many aspects from the recent proposal by Marzari and Vanderbilt.[1] First of all, it is a two-step self-consistent procedure, alternating a wannierization step applied to all **k** points and a Boys-type localization applied to the Wannier functions of the reference cell only. In the case of Marzari and Vanderbilt, on the contrary, the localization is performed through a global numerical optimization applied to all vectors at each **k** point. A second major difference is related to the basis set adopted in the SCF calculation: plane waves or atomic orbitals. Many technical aspects of the two localization schemes are intimately related to the adopted basis set.

B. Spontaneous polarization and effective Born charges

The spontaneous polarization has been evaluated in two ways.

The first way is based on the use of BF's. We refer to the original paper for the formalism[4–7] as implemented in the CRYSTAL code.[18] Essentially, we compute the spontaneous polarization as a change in BP's (Refs. 27 and 28) from the centrosymmetric to the ferroelectric structure. The main formula of the Berry phase theory for closed shell systems, due to King-Smith and Vanderbilt,[4] can be cast as

$$\Delta \mathbf{P}_{\mathrm{el}} = -\frac{i}{(2\pi)^3}\int_{BZ} d\mathbf{k}[\langle \Phi^{(1)}(\mathbf{k})|\nabla_{\mathbf{k}}\Phi^{(1)}(\mathbf{k})\rangle - \langle \Phi^{(0)}(\mathbf{k})|\nabla_{k}\Phi^{(0)}(\mathbf{k})\rangle], \tag{15}$$

where

$$|\Phi^{(\epsilon)}(\mathbf{k})\rangle = \frac{1}{\sqrt{(2N)!}}|u_1^{(\epsilon)}(\mathbf{k})\overline{u}_1^{(\epsilon)}(\mathbf{k})\cdots u_N^{(\epsilon)}(\mathbf{k})\overline{u}_N^{(\epsilon)}(\mathbf{k})| \tag{16}$$

is the Slater determinant built from the periodic parts of the CO$\psi_n^{(\epsilon)}(\mathbf{k})$,

$$u_s^{(\epsilon)}(\mathbf{k}) = \exp(-i\mathbf{k}\cdot\mathbf{r})\,\psi_s^{(\epsilon)}(\mathbf{k}), \tag{17}$$

BZ stands for the Brillouin zone, ϵ is a parameter describing the deformation from the one ($\epsilon=0$) to the other geometry ($\epsilon=1$), and N is the number of bands considered.

In practical implementation, the integral in Eq. (15) is performed over an arbitrary discrete **k**-point set. We use a uniform mesh with $L=I_1\times I_2\times I_3$ points along the primitive $\mathbf{G}_i$ reciprocal lattice vectors:

$$\mathbf{k}_{j_1j_2j_3} = \frac{j_1}{I_1}\mathbf{G}_1 + \frac{j_2}{I_2}\mathbf{G}_2 + \frac{j_3}{I_3}\mathbf{G}_3, \tag{18}$$

where $j_i=0,\ldots,I_i-1$.

In the basis of the LWF's, $\Delta\mathbf{P}_{\mathrm{el}}$ takes a much simpler form

$$\Delta \mathbf{P}_{\mathrm{el}} = \frac{1}{V}(\overline{\mathbf{r}}^{(1)} - \overline{\mathbf{r}}^{(0)}), \tag{19}$$

where V is the primitive cell volume and

$$\overline{\mathbf{r}}^{(\epsilon)} = -2\sum_{s=1}^{N}\int d\mathbf{r}\mathbf{r}|\omega_s^{(\epsilon)}(\mathbf{r})|^2. \tag{20}$$

Here the sum runs either over the occupied or valence bands.

From the $\Delta\mathbf{P}$ data, the dynamical charge tensor $\mathbf{Z}^*_{p,\alpha\gamma}$ associated with each ion p of the system can be deduced. This tensor describes the response of the system, in terms of polarization changes, to a periodic displacement $\mathbf{u}_p$ of ion p under a lattice strain γ and/or a field α. The corresponding tensor is defined as the derivative of $\Delta\mathbf{P}$ with respect to the atomic sublattice displacements:[3]

$$\mathbf{Z}^*_{p,\alpha\gamma} = V\frac{\partial \Delta\mathbf{P}_\alpha}{\partial \mathbf{u}_{p,\gamma}}. \tag{21}$$

Here, due to symmetry constraints, only the z components of $\Delta\mathbf{P}$, $\mathbf{u}_{p,\gamma}$, and Born (or transverse) effective charges[2] (without any applied electric field) are considered. The Born charges Z_p^* obey the acoustic sum rule

$$S_\alpha = \sum_p Z_p^* = 0. \tag{22}$$

These charges can be computed directly from their definition in Eq. (21), i.e., from the polarization variation induced by the displacement of each atomic sublattice. In practice, we deduce the derivative from a linear regression of the polarization variation versus the atomic displacements curve.

III. RESULTS AND DISCUSSION

A. Localized crystalline orbital of $KNbO_3$

With the basis sets defined in Sec. II (small core pseudopotentials for K and Nb) there are 22 core electrons (8 in the $3sp$ shell of K, 8 in the $4sp$ shell of Nb, and 6 in the $1s$ shell of the three oxygen atoms) and 24 valence electrons (1 for $4s$ of K, 2 for $5s$, and 3 for $4d$ of Nb, 18 for $2sp$ of the three oxygen atoms) in the unit cell corresponding to 11 core and 12 valence occupied bands. The band structure of all occupied states is reported in Fig. 1, where the characterization of bands in terms of the most widely contributing atomic orbitals is also indicated. The very large gaps between bands, the lack of any dispersion of most bands as a function of **k**, and conservation of degeneracy confirm both the core nature of the lowest bands and the very ionic nature of the compound. Only for the $2s$ and $2p$ states of oxygen is some degree of dispersion observed, and degeneracy is removed to some extent.

The main features of the LWF's, as resulting from the localization process extended to all the occupied bands, are reported in Table II. The localization indices λ^s of the LWF's corresponding to K and Nb inner electrons are very close to 1, confirming the core nature of these states. They are characterized by short distances of the centroids from the atoms indicated in the first column of Table II (0.31–0.36 Å) and quite small σ^s values, which are defined with respect to the centroid $\mathbf{r}_0^s$ as follows:

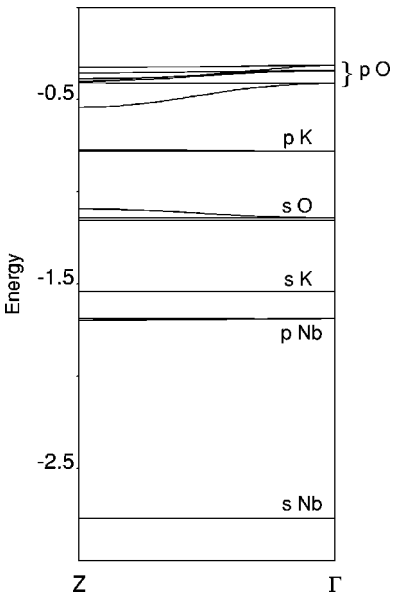

FIG. 1. Valence band structure of cubic $KNbO_3$. Energies in a.u.

$$\sigma^s = \sqrt{\int |\omega_s(\mathbf{r})|^2 (\mathbf{r}-\mathbf{r}_0^s)^2 d\mathbf{r}}. \tag{23}$$

It is interesting to notice that *s* and *p* states of K mix to give four equivalent WF's, whereas in the Nb case, probably owing to the larger energy difference, *s* and *p* do not mix very much. Also in the case of oxygen, the corresponding WF's have essentially an atomiclike character, with a localization index λ^s equal to 1.13 and 1.23 (we remind the reader that in the case of pure covalent bands, such as in bulk silicon, $\lambda^s \cong 2$). The distance from the ''reference'' atom is, however, larger in this case, as well as the corresponding σ^s values. It is worth noting that the ''extent,'' σ^s, of the largest WF (0.9 Å) is about half the Nb-O distance (2 Å).

It is also interesting to analyze the LWF's in terms of contributions to the atomic populations as defined in Eq. (6). The result of this analysis for the more diffuse LWF's is reported in Table III. These are the two WF's that are mainly localized on O_I; they will be referred to as type 1 and 2. It turns out that 94% and 89% of the electron density is localized on O_I for $\omega_{s=\text{type 1}}$ and $\omega_{s=\text{type 2}}$, respectively. When also the two nearest neighbors of O_I are considered, more than 99% of the density is obtained and 99.95% when the 10–12 most important atomic contributions are summed up. These features confirm that also these valence states are extremely localized, though not as much as in the case of the K and Nb core states, where a single atom contributes more than 99.9% of the electron density. The extremely localized nature of type 1 and 2 WF's is still more evident from Fig. 2, where the WF's themselves and their square (electron charge density) are represented. In particular, the charge density maps, in the bottom part of the figure, show that the LWF's are completely localized on O_I. Nevertheless, the small contribution from Nb in the right figure must not be neglected: it indicates some bonding character of $\omega_{\text{type 2}}$, which is at the origin of the very high value of Z^* of this atom (see below).

It is interesting to observe what happens when only a subset of bands is localized. The results are shown in Table IV. When only the highest 9 *p* oxygen states are localized (highest part of the table) the localization is incomplete, because the *p* states cannot mix with *s* states. If the second and

TABLE II. Characterization of the LWF's. For each set of N^s equivalent LWF's (ω_s), λ^s is the localization index [see Eq. (14)] d^s is the distance of the ω_s centroid from the nearest atom (first column), and σ^s is a measure of the extent of ω_s [see Eq. (23)].

Atom	N^s	$\lambda^2(e^{-2})$	d^s (Å)	σ^s (Å)
O	3	1.228	0.398	0.847
O	9	1.133	0.319	0.859
K	4	1.003	0.356	0.719
Nb	3	0.981	0.317	0.643
Nb	1	0.978	0.314	0.638

TABLE III. Characterization of $\omega_{\text{type 1}}$ and $\omega_{\text{type 2}}$ (first and second entries in Table II). $q^s_{A,\mathbf{R}_l}$ (in $|e|$) is the fraction of the total density of the ω_s attributed to atom *A* in cell *l* according to a Mulliken partition [see Eq. (6)]. Q^s is the incremental sum of the $q^s_{A,\mathbf{R}_l}$ contributions to the ω_s total charge (only contributions larger than $|0.0001\|e|$ are reported). Charge density is normalized to 1.

Type	A	$\mathbf{R}_l$	$q^s_{A,\mathbf{R}_l}$	A	$\mathbf{R}_l$	$q^s_{A,\mathbf{R}_l}$	A	$\mathbf{R}_l$	$q^s_{A,\mathbf{R}_l}$	Q^s
1	O_I	(0,0,0)	0.9380							0.9380
	Nb	(0,0,0)	0.0380	Nb	(0,0,−1)	0.0205				0.9973
	O_{II}	(0,1,0)	0.0009	O_{II}	(1,0,0)	0.0006	O_{II}	(0,0,−1)	0.0004	
	O_{II}	(0,0,0)	0.0002	Nb	(0,1,0)	0.0002	Nb	(0,1,−1)	0.0001	
	Nb	(0,−1,−1)	0.0001	O_I	(0,0,1)	0.0001	Nb	(1,1,0)	−0.0001	
	K	(1,1,0)	−0.0003							0.9995
2	O_I	(0,0,0)	0.8880							0.8880
	Nb	(0,0,−1)	0.0861	Nb	(0,0,0)	0.0179				0.9920
	$O_{II}(2)$	(0,0,−1)	0.0019	$O_{II}(2)$	(1,0,−1)	0.0018	O_I	(0,0,−1)	−0.0022	0.9972
	$O_{II}(2)$	(0,1,0)	0.0006	$O_{II}(2)$	(0,0,0)	0.0004	O_I	(0,0,1)	0.0002	
	Nb	(0,0,−2)	0.0002	Nb	(0,0,1)	0.0001				0.9997

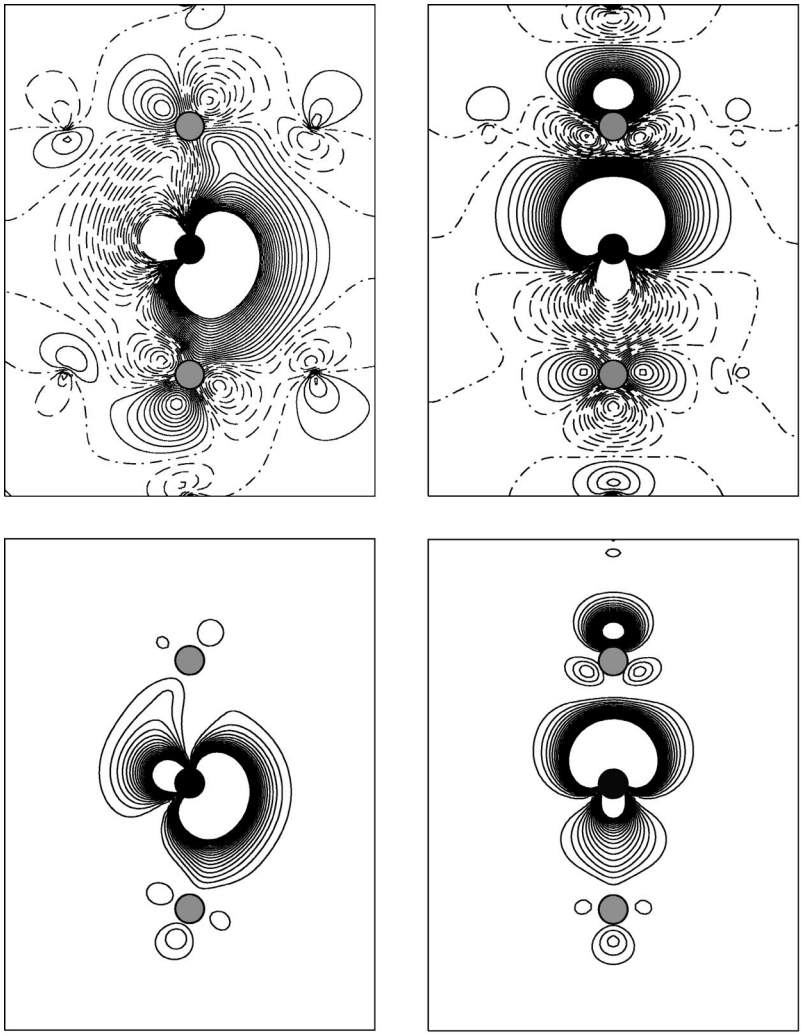

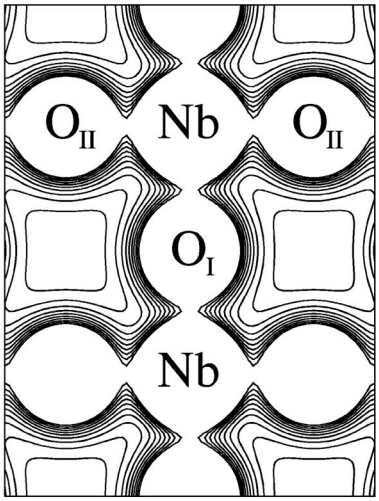

FIG. 2. Isoline representation of $\omega_{\text{type 1}}$ and $\omega_{\text{type 2}}$ (top) and the corresponding electron charge density ($|\omega_s|^2$) maps (bottom) in the (100) plane of cubic $KNbO_3$. Consecutive isolines differ by 0.005 bohr$^{-3/2}$ in the maps of ω_s and by 0.001 e/bohr^3 in the isodensity maps. Solid, dashed, and dot-dashed lines denote positive, negative, and zero values. Dark and pale gray circles mark the O_I and Nb nuclei, respectively. The total charge density map in the same section is reported below for reference (0.01 e/bohr^3 between isolines).

third sets of states from top are also included, namely, the p_K and s_O states, the resulting WF's are extremely close to the ones obtained with the full set. When also the p Nb states are included in the localization, only marginal differences in the indices λ^s, σ^s, and $q^s_{A,\mathbf{R}}$ are observed with respect to a localization of all the occupied orbitals.

B. Spontaneous polarization and related quantities

As had been pointed out since the pioneering papers by King-Smith and Vanderbilt[4] and Resta,[5–7] important physical properties such as the effective Born charges Z^* and the spontaneous polarization $\Delta\mathbf{P}$ take an extremely simple expression in terms of the LWF's. In the delocalized BF basis,

TABLE IV. Evolution of the WF characteristics λ^s, σ^s, and $q^s_{A,\mathbf{R}}$ (see Tables II and III for definition) as a function of the number M of bands involved in the localization process. N_s is the number of equivalent ω_s functions. In all cases, the M BF's with higher energy are considered ($M=10$ in Table II).

M	Atom	N_s	$\lambda^s(e^{-2})$	σ^s (Å)	$q^s_{A,\mathbf{R}}(\lvert e\rvert)$
9	O	3	1.317	1.088	0.867
		3	1.254	1.061	0.891
		3	1.166	1.021	0.925
15	O	6	1.253	0.897	0.889
		6	1.137	0.922	0.937
	K	3	1.004	0.822	0.998
19	O	3	1.240	0.848	0.895
		9	1.135	0.862	0.938
	K	4	1.003	0.718	0.999
	Nb	3	0.982	0.732	1.009

on the contrary, things are more complicated and the calculation of both these quantities became possible only with the elegant formulation of the BP approach by King-Smith and Vanderbilt[4] in 1993. As a matter of fact, both formulations are expected to provide the same results, in principle. In practice all technical details related to the specific implementations will introduce a certain amount of error that is difficult to determine *a priori*. In this section, we compare the Z^* and $\Delta\mathbf{P}$ data for $KNbO_3$ as obtained by these two alternative methods. In Table V, the values of $\Delta\mathbf{P}$ are reported as a function of the shrinking factors I_1, I_2, I_3 for the three reciprocal lattice vectors. The ΔP_x and ΔP_y components are expected to be zero by symmetry and, as point symmetry is not imposed on the system in either scheme, the deviation of ΔP_x and ΔP_y from zero is a measure of numerical noise. It turns out that for $I_1=I_2=I_3=12$ it is on the order of 10^{-6} with the LWF approach, whereas it is much smaller (10^{-16}) with BP's. Nevertheless, as regards ΔP_x, the two methods

TABLE V. Dependence of the spontaneous polarization vector $\Delta\mathbf{P}$ (in C/m^2) on the shrinking factors, I_1, I_2, I_3 defining the reciprocal space mesh as evaluated through BP and LWF. N is the corresponding number of $\mathbf{k}$ points in the irreducible Brillouin zone. The experimental geometry (Ref. 25) has been used. $x(-y)$ stands for $x\times10^{-y}$. The experimental value of $\Delta\mathbf{P}$ is 0.37 C/m^2.

	$I_1I_2I_3$	N	ΔP_x	ΔP_y	ΔP_z
BP	2 2 2	6	6(−16)	0.	0.3199
	4 4 4	18	3(−16)	3(−16)	0.3296
	4 4 8	30	1(−16)	1(−16)	0.3340
	4 4 12	42	1(−16)	8(−17)	0.3348
	8 8 8	75	2(−15)	1(−15)	0.3339
	8 8 12	105	6(−16)	8(−16)	0.3347
LWF	4 4 4	18	3(−3)	3(−3)	0.3378
	8 8 8	75	3(−5)	3(−5)	0.3362
	12 12 12	196	6(−6)	6(−6)	0.3361

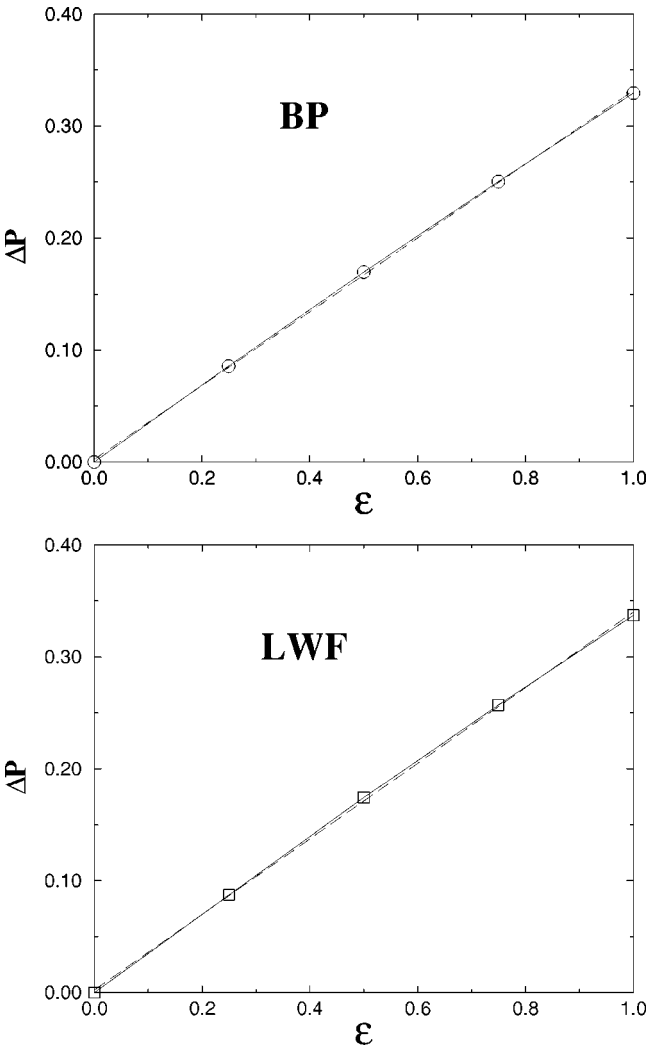

FIG. 3. Spontaneous polarization (ΔP, in C/m^2) as a function of the ferroelectric distortion ϵ when the BP (top, circles) or the LWF (down, squares) schemes are used. $\epsilon=1$ corresponds to the experimental geometry of the ferroelectric structure at 270 °C (Ref. 25). The dashed line is obtained by linear interpolation of $\Delta\mathbf{P}$ in the $0\leqslant\epsilon\leqslant1$ interval. The shrinking factors are $I_1=I_2=I_3=4$.

agree to within the third decimal (which corresponds to a 0.2% difference) and the LWF scheme converges much more rapidly than BP's with increasing the shrinking factors.

Further evidence of the equivalent accuracy of the two schemes is provided by Table VI and Fig. 3. The values of Z^* reported in the table for all atoms are obtained from Eq. (21). Both methods provide Z^* values that differ by $10^{-3}|e|$

TABLE VI. Born effective charges Z^* (in $|e|$), acoustic sum rule S_a (in $|e|$), and $\Delta P_{\rm tot}$ (in C/m^2) obtained by using the BP and LWF schemes. $I_1=I_2=4$, $I_3=12$ and $I_1=I_2=I_3=8$ have been used for the BP and LWF calculations, respectively.

Method	$Z^*_{\rm Nb}$	Z^*_K	$Z^*_{O_I}$	$Z^*_{O_{II}}$	S_a	$\Delta P_{\rm tot}$
BP	8.073	1.001	−5.964	−1.556	−0.0003	0.347
LWF	8.089	1.000	−5.985	−1.552	0.0004	0.348

on average (the largest difference is observed for O_I and amounts to 0.4% $Z^*_{O_I}$). The deviation from the sum rule [Eq. (22)] is on the order of 10^{-4} and very similar values of the total polarization

$$\Delta P_{\text{tot}} = \sum_A Z^*_A u_A \tag{24}$$

are also obtained, which differ only by about 0.3%. Figure 3 represents ΔP as a function of ϵ, the degree of deformation of the lattice from the symmetric ($\epsilon=0$) to the experimental ($\epsilon=1$) deformed geometry. It shows that the two approaches agree not only at the experimental deformation ($\epsilon=1$) but also for much smaller ϵ values and the curve is perfectly linear in the full range.[29–31]

IV. CONCLUSIONS

It has been shown that the recently implemented localization scheme in the CRYSTAL program[19] is not only a useful tool for the interpretation of the electronic structure of crystalline compounds in terms of chemical-like concepts, but it can be applied for economical and accurate evaluations of important physical properties such as Z^* charges and the spontaneous polarization $\Delta\mathbf{P}$, as a valuable alternative to the BP approach. Both computational approaches will be available in the forthcoming release of the CRYSTAL package, CRYSTAL2001.

ACKNOWLEDGMENTS

This research has been supported by the European Community program ''Improving Human Potential and the Socio-economic Knowledge Base'' under Contract No. HPMF-CT-1999-0380. C.Z. thanks the University of Turin for a grant.

*Permanent address: Departamento de Física, Universidad Autónoma del Estado de Morelos, Av. Universidad 1001, Col. Chamilpa, 62210 Cuernavaca (Morelos), Mexico.

†To whom correspondence should be addressed. Electronic address: dovesi@ch.unito.it

[1] N. Marzari and D. Vanderbilt, Phys. Rev. B **56**, 12 847 (1997).
[2] R. Pick, M. H. Cohen, and R. M. Martin, Phys. Rev. B **1**, 910 (1970).
[3] Ph. Ghosez, J. P. Michenaud, and X. Gonze, Phys. Rev. B **58**, 6224 (1998).
[4] R. D. King-Smith and D. Vanderbilt, Phys. Rev. B **47**, 1651 (1993).
[5] R. Resta, Ferroelectrics **136**, 51 (1992).
[6] R. Resta, Europhys. Lett. **22**, 133 (1993).
[7] R. Resta, Rev. Mod. Phys. **66**, 809 (1994).
[8] S. Diner, J. P. Malrieu, P. Claverie, and F. Jordan, Chem. Phys. Lett. **2**, 319 (1968).
[9] P. Pulay, Chem. Phys. Lett. **100**, 151 (1983).
[10] Martin Schütz, Georg Hetzer, and Hans-Joachim Werner, J. Chem. Phys. **111**, 5691 (1999).
[11] P. J. Knowles, M. Schütz, and H. J. Werner, in *Ab Initio Methods for Electron Correlation in Molecules*, edited by Johannes Grotendorst, *Modern Methods and Algorithms of Quantum Chemistry*, Proceedings, 2nd ed. (NIC, 2000), Vol. 3.
[12] Martin Schütz and Hans-Joachim Werner, J. Chem. Phys. **114**, 661 (2001).
[13] S. F. Boys, Rev. Mod. Phys. **32**, 296 (1960).
[14] J. M. Foster and S. F. Boys, Rev. Mod. Phys. **32**, 300 (1960).
[15] C. M. Zicovich-Wilson, R. Dovesi, and V. R. Saunders (unpublished).
[16] J. Pipek and P. G. Mezey, J. Chem. Phys. **90**, 4916 (1989).
[17] Ph. Millié, B. Lévy, and G. Berthier, in *Localization and Delocalization in Quantum Chemistry*, edited by Chalvet *et al.* (Reidel, Dordrecht, 1975), Vol. 1.
[18] S. Dall'Olio, R. Dovesi, and R. Resta, Phys. Rev. B **56**, 10 105 (1997).
[19] V. R. Saunders, R. Dovesi, C. Roetti, M. Causa, N. M. Harrison, R. Orlando, and C. M. Zicovich-Wilson, *CRYSTAL98 User's Manual* (Università di Torino, Torino, 1998).
[20] P. J. Hay and W. R. Wadt, J. Chem. Phys. **82**, 270 (1985).
[21] P. J. Hay and W. R. Wadt, J. Chem. Phys. **82**, 284 (1985).
[22] P. J. Hay and W. R. Wadt, J. Chem. Phys. **82**, 299 (1985).
[23] M. P. Habas, R. Dovesi, and A. Lichanot, J. Phys.: Condens. Matter **10**, 6897 (1998).
[24] Variational basis sets are available at the following web site: http://www.ch.unito.it/ifm/teorica/Basis_Sets/mendel.html.
[25] A. W. Hewat, J. Phys. C **6**, 1074 (1973).
[26] H. J. Monkhorst and J. D. Pack, Phys. Rev. B **13**, 5188 (1976).
[27] J. Zak, Phys. Rev. Lett. **62**, 2747 (1989).
[28] L. Michel and J. Zak, Europhys. Lett. **18**, 239 (1992).
[29] C. Z. Wang, R. Yu, and H. Krakauer, Phys. Rev. B **54**, 11 161 (1996).
[30] W. Kleemann, F. J. Schäfer, and M. D. Fontana, Phys. Rev. B **30**, 1148 (1984).
[31] M. D. Fontana, G. Métrat, J. L. Servoin, and F. Gervais, J. Phys. C **17**, 483 (1984).